The Rb-Sr (Rubidium-Strontium) System

85.4678 87.62

By A. D. Pelton
Ecole Polytechnique de Montréal

The Rb-Sr system was found by Klemm and Kunze [67Kle] to exhibit virtually complete immiscibility in both solid and liquid states. No compounds were found by X-ray diffraction.

Crystal structure and lattice parameter data are given in Table 1.

Cited Reference

*67Kle: W. Klemm and D. Kunze, "Systems of Alkali and Alkaline Earth Metals," Proc. Int'l. Symp. on Alkali Metals, London Chem. Soc., Special Publ. No. 22, 3-22 (1967). (Equi Diagram; Experimental; #)

*Indicates key paper.
#Indicates presence of a phase diagram.

Table 1 Rb-Sr Crystal Structure and Lattice Parameter Data

Phase	Composition, at.% Sr	Pearson symbol	Space group	Prototype	Lattice parameter, nm a	Comment	Reference
(Rb)	0	*cI*2	*Im*3*m*	W	0.5703	At 25 °C	[King1]
(αSr)	100	*cF*4	*Fm*3*m*	Cu	0.6084	At 25 °C	[King1]
(γSr)(a)	100	*cI*2	*Im*3*m*	W	0.485	At 614 °C	[Pearson2]

(a) Above 557 °C.

Rb-Sr contributed by **A. D. Pelton,** Centre de Recherche en Calcul Thermochimique, Ecole Polytechnique, Campus de l'Université de Montréal, P.O. Box 6079, Station A, Montréal, Québec, Canada H3C 3A7. This work was (partially) supported by the United States Department of Energy funds through the Joint Program on Critical Compilation of Physical and Chemical Data coordinated through the Office of Standard Reference Data, National Bureau of Standards. Literature searched through 1983. Dr. A. D. Pelton is the ASM/NBS Data Program Co-Category Editor for binary alkali systems.

The Au-Pt (Gold-Platinum) System

196.9665 195.08

By H. Okamoto and T. B. Massalski
Carnegie-Mellon University

The equilibrium phases of the Au-Pt system are: (1) the liquid, L; and (2) the fcc, continuous solid solution, (Au, Pt), encompassing a miscibility gap (Au) + (Pt). The critical point of the miscibility gap is at about 61 at.% Pt and 1260 °C. The solid phase boundaries in Fig. 1 have been drawn according to the experimental data of [52Dar] as well as a tentative thermodynamic model similar to that of [71Kub]. The liquid phase boundaries were drawn from a subregular solution model derived from the experimental boundaries of [07Doe], [28Gri], [30Joh], [31Ste], [38Wic], [47Wic1], [47Wic2], [49Wic], [51Gru], [52Dar], [57Tie], [60Mun], and [64Rau]. Experimental data are not sufficient to establish a completely satisfactory thermodynamic model, but the features shown in Fig. 1 may only differ in very small detail from a true representation for this system. Earlier reviews were published by [62Dar], [78Sav], and [81Sin].

Equilibrium Diagram

The Au-Pt phase diagram has been investigated extensively because of the experimental and theoretical interest in the miscibility gap occurring in the solid solution field, as well as the controversy regarding the form of the liquidus and solidus boundaries. Very early reports on this system, as early as in 1796, concerning the alloying characteristics are summarized in the review paper by [62Dar]. [07Doe] concluded from cooling curves using six alloys that a continuous series of solid solutions can be obtained following crystallization from the melt. The miscibility gap in the solid state was first observed by [30Joh], who used mainly resistivity measurements. Many supporting reports with better accuracy and more detail followed this work. In the mean time, probably misguided by the nearly horizontal form of the solidus (Fig. 1), [28Gri] and [51Gru] proposed a diagram with a peritectic reaction L + (Pt) → (Au). This was proved not to be true by [52Dar] from detailed thermal, microscopic, X-ray, and resistivity observations.

Liquidus. The melting points of Au and Pt are accepted as 1064.43 °C and 1769.0 °C, respectively [Melt]. All the liquidus data by [07Doe], [28Gri], [51Gru], and [52Dar] given in Table 1 were determined from cooling curves. Agreement between these data is fairly good, as can be seen in Fig. 1, although the melting point of Pt by [07Doe] and [28Gri] is considerably lower than the accepted value and a large experimental scatter can be seen in the data of [28Gri]. The liquidus line in Fig. 1 is based on the experimental data of [52Dar].

Solidus. The solidus data were obtained by [07Doe], [28Gri], and [51Gru] from cooling curves, by [47Wic2] and [51Gru] from electrical resistivity vs temperature curves,

Fig. 1 Assessed Au-Pt Phase Diagram

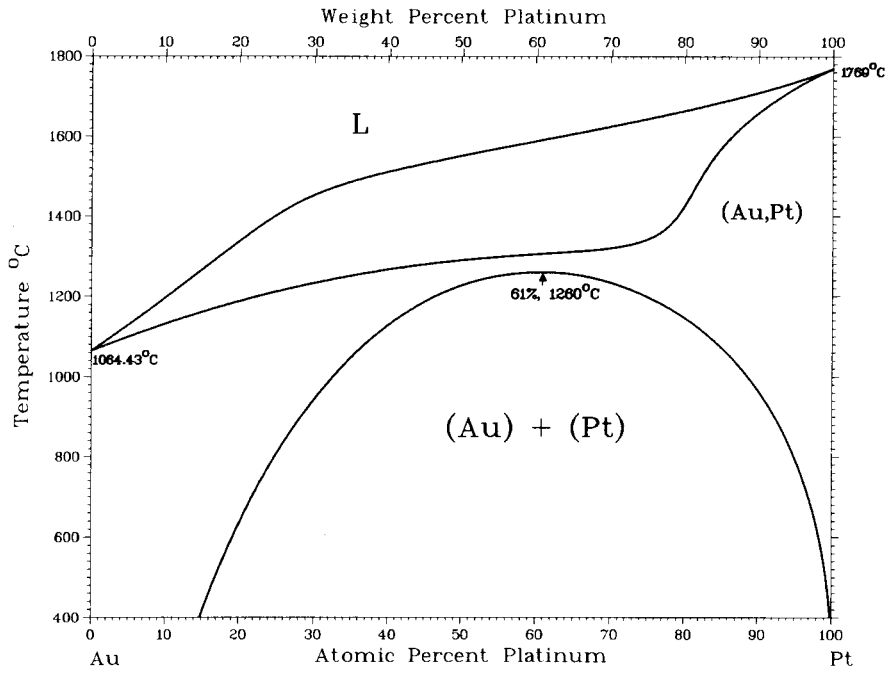

(a)

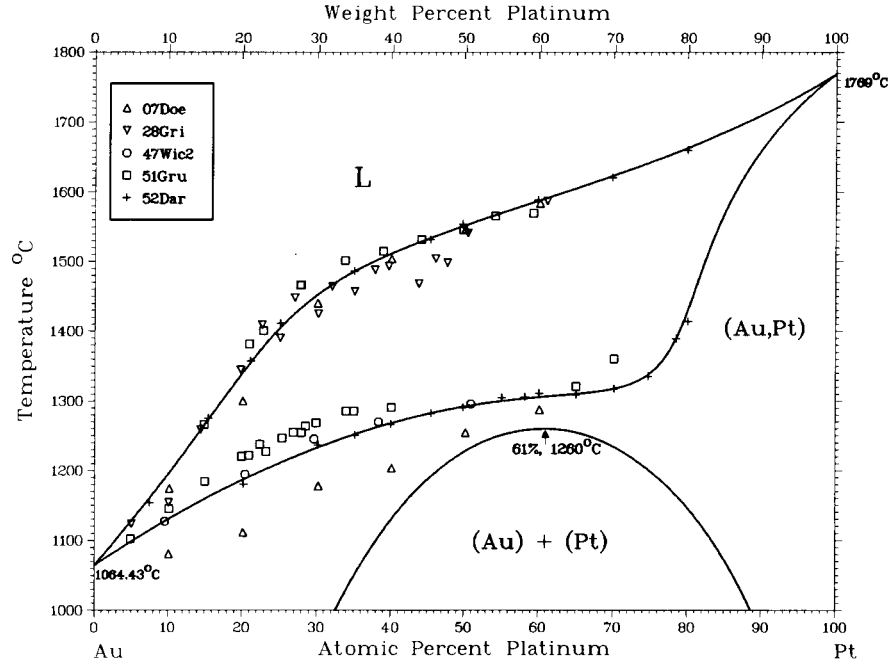

(b)

(**a**) Assessed diagram. (**b**) Assessed liquidus and solidus. H. Okamoto and T. B. Massalski, 1985.

Fig. 1 Assessed Au-Pt Phase Diagram (continued)

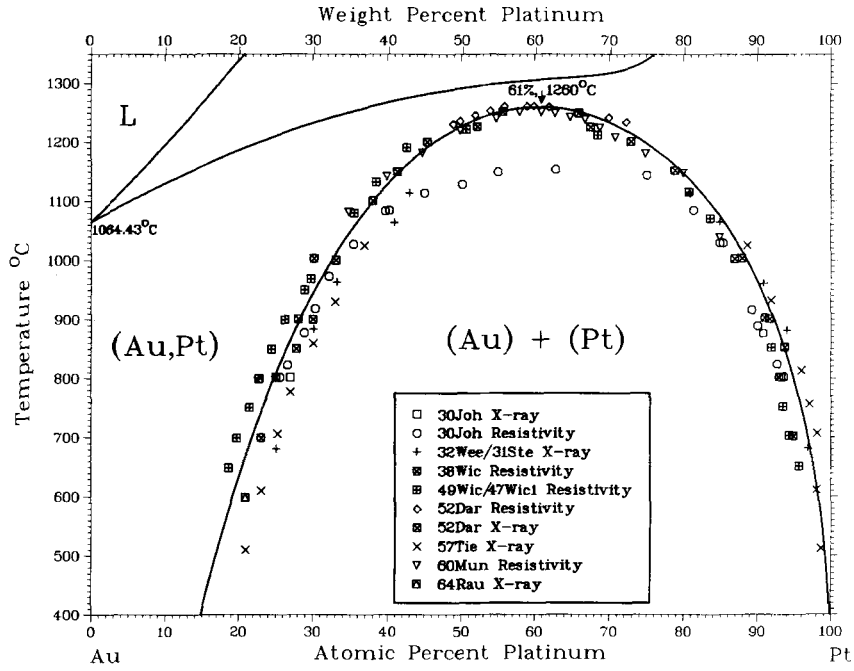

(c)

(c) Assessed miscibility gap.

H. Okamoto and T. B. Massalski, 1985.

Table 1 Experimental Data on Liquidus

Composition, at.% Pt	Temperature, °C	Composition, at.% Pt	Temperature, °C
[07Doe]		**[28Gri] (cont'd)**	
0	1064	22.7	1410
10.1	1174	25.2	1389
20.2	1299	27.2	1447
30.2	1437	30.17	1425
40.2	1503	32.2	1462
50.2	1544	35.2	1456
60.2	1579	37.86	1487
100	1744	39.98	1493
[52Dar]		44.09	1467
7.6	1155	46.11	1502
15.1	1274	47.7	1496
20.21	1355	50.59	1540
25.2	1408	61.54	1582
35.2	1483	100	1755
45.47	1529	**[51Gru]**	
49.95	1550	10.2	1197
60.2	1584	15.0	1266
69.94	1617	21.0	1382
80.2	1655	23.0	1401
[28Gri]		28.0	1466
0	1063	34.0	1502
5.0	1123	38.9	1513
10.14	1154	44.3	1530
15.1	1259	50.0	1544
19.91	1345	54.4	1562
		59.3	1569

Table 2 Experimental Data on Solidus

Composition, at.% Pt	Temperature, °C	Composition, at.% Pt	Temperature, °C
[07Doe] (a)		**[47Wic2] (cont'd)**	
10.1	1079	29.5	1245
20.2	1109	38.5	1270
30.2	1177	51.0	1294
40.2	1203	**[51Gru] (a)**	
50.2	1253	10.2	1149
60.2	1285	15.0	1188
[52Dar] (b)		21.0	1223
20.21	1180.5 ± 2.5	23.0	1229
30.22	1235	28.0	1255
35.2	1249.5	34.0	1286
40.2	1265	65.2	1314
45.47	1280	70.0	1357
49.95	1287.5	**[51Gru] (c)**	
55.2	1302.5	5	1105
58.2	1302.5	10	1147
60.2	1307.5	15	1187
65.2	1307.5	20	1219
69.94	1312.5	22.5	1240
74.72	1332.5	25	1247
78.03	1369.5	26.7	1254
80.2	1410	28.4	1263
[47Wic2] (c, d)		30	1267
9.6	1128	35	1285
20.4	1196	40	1290

(a) Thermal. (b) Microscopic. (c) Electrical Resistivity. (d) From [Hansen].

and by [52Dar] from microscopic observations. The data by [07Doe], [47Wic2], [51Gru], and [52Dar] are listed in Table 2. The data by [28Gri] and part of the data by [51Gru] were omitted here because of the large experimental uncertainty involved, which presumably lead to the erroneous conclusion about the occurrence of a peritectic reaction. The solidus temperatures by [07Doe] are too low, an error often encountered when the cooling curve method is employed. The solidus line in Fig. 2 is based on

Fig. 2 Au-Pt Spinodal Curve

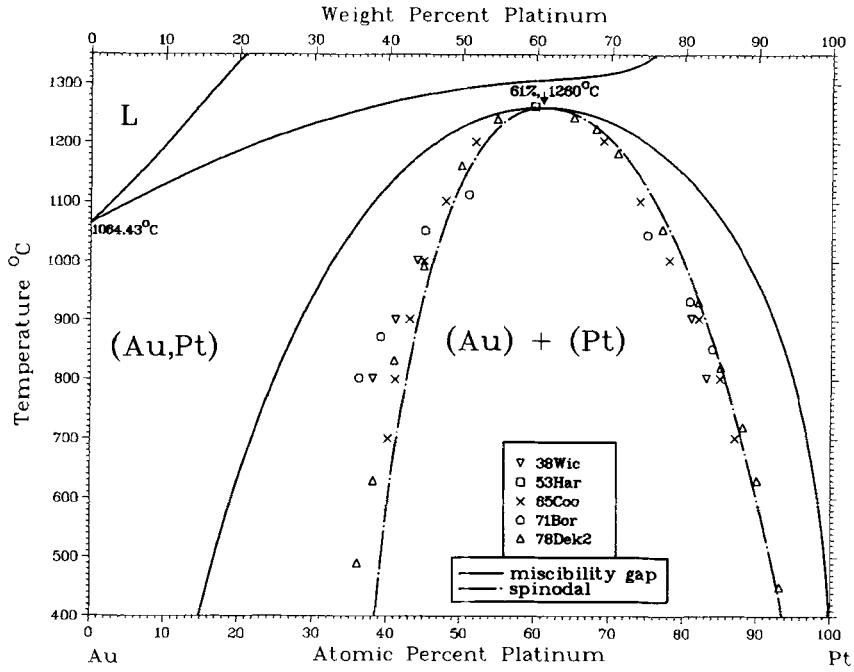

Solid line is based on the present thermodynamic model. H. Okamoto and T. B. Massalski, 1985.

the data of [52Dar] for 0 to 80 at.% Pt and on the present thermodynamic model for 80 to 100 at.% Pt.

Incoherent Miscibility Gap. The incoherent (stable) miscibility gap in the solid state was experimentally observed mainly with electrical resistivity measurements [30Joh, 38Wic, 47Wic1, 49Wic, 52Dar, 60Mun] and X-ray measurements [30Joh, 31Ste(32Wee), 51Gru, 52Dar, 57Tie, 64Rau] (Table 3, Fig. 1). The earliest studies of resistivity in quenched alloys by [30Joh] indicated a fairly low critical temperature (~1150 °C) when compared with later experiments (~1260 °C), probably due to the insufficient quenching rate employed by [30Joh]. Later resistivity measurements carried out at high temperatures agreed with one another reasonably well (see Fig. 1). The miscibility gap boundary determinations with X-ray methods also are in generally good agreement. The composition corresponding to the critical temperature is about 61 at.% Pt. The miscibility gap curve in Fig. 1 is based on the present thermodynamic model.

Spinodal curves associated with the observed miscibility gap can be estimated from experimental data using different models or assumptions. These were discussed by [38Wic], by [65Coo] from the data of [52Dar] and [57Tie], by [71Bor] from the data of [49Wic], and by [78Dek2] from the van der Waals differential equation for coexisting phases and with assumed ideal entropy of mixing (Table 4). Some ambiguity regarding the shape of the spinodal is inevitable (Fig. 2). The spinodal can be also determined theoretically (see "Thermodynamics"). The kinetics of formation of the miscibility gap have been discussed by [37Joh], [38Bor], [38Wic], [51Bor], [60Too2], [67Car], [70Kra], [78Dek1], and [78Sin2].

Crystal Structures

The lattice parameters of pure Au and Pt at 25 °C are accepted as 0.40784 nm [King1] and 0.39233 nm [King1] an obvious misprint in the table of lattice parameters has been corrected]. The Au-Pt system has only one stable structure (Au, Pt) based on the Cu-type fcc solid solution. The lattice parameters of the quenched alloys were measured by [30Joh], [51Gru], [52Dar], [55Rau], and [67Car] (Table 5). Annealing temperatures seem to have little effect on the lattice parameter (within experimental error). The deviation from an assumed Vegard's law is very slight (Fig. 3). Short-range order in dilute Pt alloys has been observed in 98 at.% Pt alloys [68Gol], and 96 and 99.38 at.% Pt alloys by [75Che]. The results by the latter for the 99.38 at.% Pt alloy may be incorrect [76Mac].

Metastable Phases

Intermetallic Compounds. The Au_3Pt phase is classified as a metastable phase here, although a definite conclusion on this has not yet been determined. The existence of this phase together with the AuPt and $AuPt_3$ phases was hinted at by [30Joh] on the basis of the change of slope in the magnetic susceptibility vs temperature curve. [51Gru] reported that the X-ray patterns showed the existence of the Au_3Pt superlattice in alloys up to 40 at.% Pt after severe cold working followed by annealing at 900 °C. [64Rau] also reported two distinguishable lattice parameters in alloys with up to ~22 at.% Pt (phase boundary) at 600 and 800 °C. On the other hand, X-ray diffraction studies of 10 and 25 at.% Pt alloys by [61San] showed that the Au_3Pt, AuPt, and $AuPt_3$ phases materialized as metastable phases during the heating of a two-phase mixture of (Au) and (Pt). [51Gru] could not confirm the existence of

Table 3 Experimental Data on the Miscibility Gap

Composition, at.% Pt	Temperature, °C	Composition, at.% Pt	Temperature, °C	Composition, at.% Pt	Temperature, °C	Composition, at.% Pt	Temperature, °C
[30Joh](a)		**[52Dar](a)**		**[57Tie](b, c)**		**[64Rau](b, c)**	
25.5	800	49.2	1229	21.2	510	21	600
26.4	820	50.2	1238	23.2	610	23	800
28.7	875	52.2	1244	25.2	705	**[47Wic1]; [49Wic](a)**	
30.2	916	58.2	1252	27.2	755	18.7	650
35.5	1025	59.2	1260	30.2	810	20.0	700
39.5	1060	60.2	1258	33.2	930	21.7	750
81.3	1060	62.2	1257	37.2	1025	23.0	800
85.0	1025	65.2	1248	89.1	1025	24.5	850
89.4	916	70.2	1243	92.1	930	26.5	900
90.8	875	72.7	1233	96	810	29.0	950
92.7	820	**[52Dar](b)**		97	755	30.0	970
93.7	800	27.9	850	98	705	36	1080
32	968	29.1	900	98	610	39	1130
40	1080	33.6	1000	99	510	45	1190
45	1108	38.5	1100	**[60Mun](a, c, d)**		51	1220
50	1125	41.8	1150	35.23	1080	60	1235
55	1145	47.0	1200	40.24	1140	69	1210
65	1150	52.8	1225	45.25	1180	75	1180
75	1140	56.3	1250	50.25	1217	81	1115
85	1025	66.4	1250	55.25	1238	84	1070
90	912	67.9	1225	58.25	1250	87	1005
[30Joh](b)		73.4	1200	61.24	1249	90	930
26.8	800	79.1	1150	63.24	1248	91.0	900
93.5	800	83.3	1100	65.23	1242	92.0	850
[31Ste]; [32Wee](b, c)		87.1	1000	67.22	1237	93.0	800
		91.9	900	69.22	1226	93.5	750
25	680	93.8	850	71.21	1208	94.5	700
30	880	**[38Wic](a)**		75.19	1180	95.5	650
33	960	23	700	80.16	1148		
41	1060	25	800	85.13	1035		
43	1110	28	900				
81	1110	30	1000				
85	1060	88	1000				
91	960	91	900				
94	880	93	800				
97	680	95	700				

(a) Resistivity measurement. (b) X-ray measurement. (c) Read from graphs. (d) Same data points in different figures show ~5 °C error.

Fig. 3 Trend of Lattice Parameters with Composition (at.% Pt) in the Au-Pt System

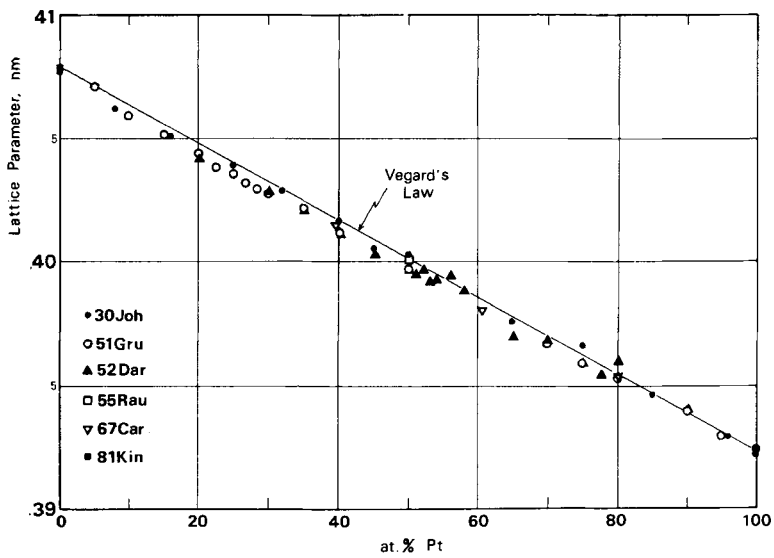

H. Okamoto and T. B. Massalski, 1985.

the AuPt and $AuPt_3$ superlattices. [57Tie] detected no diffraction lines from a second phase or superlattice lines in a 10.1 at.% Pt alloy. However, they found sidebands, reportedly related to either a pre-precipitation or a superlattice, in alloys containing 40.2 and 80.2 at.% Pt. Similar sidebands were observed by [67Fie] in 11.3 and 22.9 at.% Pt alloys. Field-ion microscopy work on the Au-Pt alloy series by [74Pol] indicated that an alloy of composition Au_3Pt is ordered when quenched from 950 °C and disordered when quenched from 1050 °C. These facts suggest that the existence of ordered structures (such as Au_3Pt, AuPt, or $AuPt_3$) is observed convincingly only in transient states, or in thin films. Crystal structures of these stoichiometric compounds are listed in Table 6.

Coherent Miscibility Gap. The coherent (metastable) miscibility gap in the solid state was observed experimentally by [68Wei] and [69Kra]. The spinodal curve associated with the coherent miscibility gap determined by [70Kra] was treated theoretically by [80Sin] (see [81Sin]).

Amorphous Phase. [78Sin1] reported the formation of an amorphous phase by implantation of Au^- ions into the platinum matrix.

Table 4 Experimental Data on Incoherent Spinodal

Composition, at.% Pt	Temperature, °C	Composition, at.% Pt	Temperature, °C
[38Wic]		**[65Coo] (cont'd)**	
38	800	52	1200
41	900	69	1200
42	1000	74	1100
76	1000	78	1000
81	900	82	900
83	800	85	800
[71Bor] (a)		87	700
36	800	**[78Dek2] (a)**	
39	870	36	490
45	1050	38	680
51	1110	41	830
75	1040	45	990
81	930	50	1160
84	850	55	1240
[65Coo] (a)		65	1240
40	700	68	1220
41	800	71	1180
43	900	77	1050
45	1000	82	930
48	1100	85	820
		88	720
		90	630
		93	450

(a) Read from graphs.

Thermodynamics

Thermodynamic Data. The only relevant experimental thermodynamic data for a phase diagram calculation were measured by [70Jon], who used a mass spectrometric method for the solid phase in the temperature range 1340 to 1520 K. The excess Gibbs energy evaluated by [Hultgren, Binary] from the data of [70Jon] and the enthalpy of mixing by [70Jon] are shown in terms of the usual function $\Delta G^{ex}/X(1-X)$ and $\Delta H/X(1-X)$ in Fig. 4 and 5, respectively, where X represents the atomic fraction of Pt in the alloys. The heat of formation values proposed by [71Hay] from high-temperature calorimetric measurements in ternary Au-Pd-Pt alloys suggest that

Table 5 Experimental Data on the Lattice Parameter

Composition, at.% Pt	Lattice parameter, nm	Composition, at.% Pt	Lattice parameter, nm
[30Joh](a)		**[51Gru](cont'd)**	
0	0.4077	40	0.40121
8	0.4062	50	0.39969
16	0.4051	70	0.39669
25	0.4039	75	0.39587
32	0.4029	80	0.39527
40	0.4017	90	0.39376
45	0.4006	95	0.39292
50	0.4003	100	0.39236
65	0.3976	**[67Car]**	
75	0.3966	39.65	0.4015
85	0.3946	60.78	0.3980
90	0.3938	80.15	0.3954
96	0.3929	**[52Dar]**	
100	0.3922	20.2	0.40416
[55Rau]		30.2	0.40280
50.3	0.4001	35.2	0.40201
[51Gru](a)		40.2	0.40119
0	0.40783	45.2	0.40026
5	0.40706	50.2	0.39963
10	0.40594	51.2	0.39950
15	0.40515	52.2	0.39967
20	0.40442	53.2	0.39916
22.5	0.40381	54.2	0.39923
25	0.40353	56.2	0.39941
26.7	0.40321	58.2	0.39980
28.4	0.40295	65.2	0.39700
30	0.40279	70.2	0.39685
35	0.40216	75.2	0.39590
		77.7	0.39543
		80.2	0.39595
		90.1	0.39389

(a) Although the original data are given in 10^{-8} cm, it is likely to be in kX units. A factor of 0.100202 was used to convert to nanometers.

Table 6 Au-Pt Crystal Structure and Lattice Parameter Data

Phase	Composition range(a), at.% Pt	Prototype	Lattice parameters, nm a	c	Comment	Reference
Metastable phases						
Au_3Pt	5 to 40	$AuCu_3$-type	0.3880	...	5 at.% Pt	[51Gru]
			0.3901	...	15 at.% Pt	
			0.3926	...	25 at.% Pt	
			0.3928	...	35 at.% Pt	
AuPt	50	...	0.3920	0.3900	(b)	[61San]
$AuPt_3$	75	...	0.3920	...	...	[61San]

(a) From the phase diagram. (b) Tetragonal.

Fig. 4 Comparison of Composition Dependence of $\Delta G^{ex}/X(1 - X)$ at 1150 °C

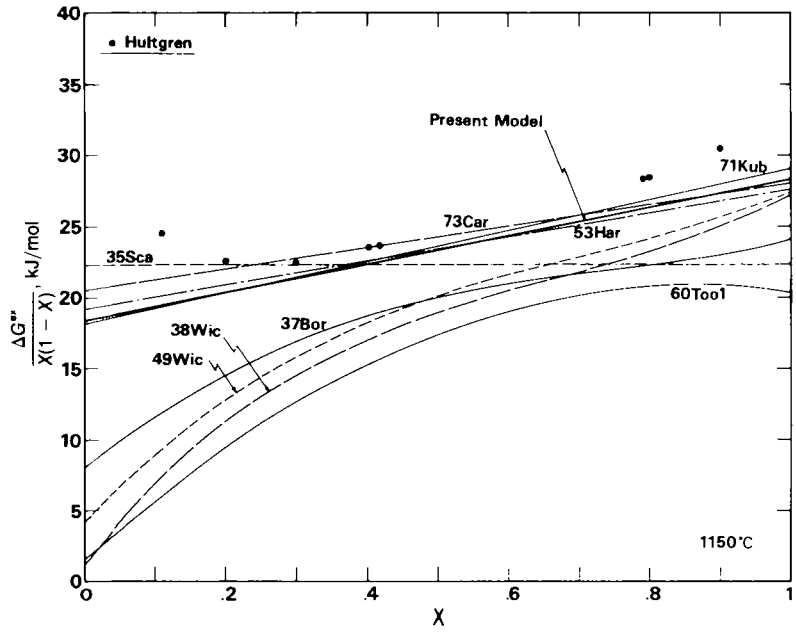

X is the atomic fraction of Pt.

H. Okamoto and T. B. Massalski, 1985.

the binary Au-Pt section should follow the relationship $\Delta H = X(1 - X)(23\,860 - 11\,930X)$ J/mol. This form is rather difficult to accept (see Fig. 5). The ΔH value deduced from short-range order coefficients by [76Mac] is also shown in Fig. 5.

No data are available for the liquid phase.

Earlier Thermodynamic Evaluations. Because the Au-Pt system is associated with a typical phase diagram involving both a continuous solubility in the solid phase and a miscibility gap in the same phase at lower temperatures, many models have been proposed in the process of developing suitable thermodynamic approaches to phase diagram calculations [34Sel, 35Sca, 35Sel, 37Bor, 38Wic, 49Wic, 52Har, 53Har, 58Wei, 60Tool, 71Kub, 73Car, 79Mul, 79Sch, 80Mie, 80Ovc, 81Pel]. The proposed thermodynamic functions for both liquid and solid phases are summarized in Table 7 in terms of the enthalpy and excess entropy of mixing. Most of the modeled functions were derived from experimental phase boundaries. [58Wei] attempted to explain the asymmetry of the miscibility gap on the basis of electronic and lattice specific heats. However, [61Mei] noted that the model by [58Wei] is incorrect. Although the Gibbs energy function of [60Tool] gives reasonable forms of phase boundaries and spinodal curves, [65Def] found a calculation error in the original paper. A seemingly correct set of coefficients resulted in an unacceptable form of the Gibbs energy curve. A model for the solid phase by [71Kub] was derived from the thermodynamic data of [70Jon]. The Gibbs energy function calculated by [79Mul] from a nearest-neighbor interaction model failed to reproduce the miscibility gap. [79Sch] estimated the contributions to the excess Gibbs energy of the solid phase by separating them into an electronic part and a lattice distortion part and obtained the following expression:

$$\Delta G^{ex}_{Au} - \Delta G^{ex}_{Pt} = -6w + 12RT \ln\{2X/(1 - 2(1 - X)T\beta)\} + K_1(1 - X) + K_2(1 - X)^2 + K_3(1 - X)^3$$

where $w = -5.53$ kJ/mol, $\beta = [1 - 4X(1 - X)(1 - \exp(-w/RT))]^{1/2}$, $K_1 = 4.0$ kJ/mol, $K_2 = -9.3$ kJ/mol, $K_3 = 22.7$ kJ/mol. [80Ovc] introduced the effect of short-range order into a model Gibbs energy function. However, the resulting phase diagram is of a peritectic form. The semiempirical model for the liquid phase proposed by [80Mie] suggests that the deviation from the regular solution is not significant. [81Pel] also suggested that the liquid phase is approximately regular. Modeled ΔG^{ex} functions for the solid phase at 1150 °C by [35Sca], [37Bor], [38Wic], [49Wic], [53Har], [60Tool], [71Kub], and [73Car] together with the experimental value of [70Jon] compiled by [Hultgren, Binary] are shown in Fig. 4. The values by [79Sch] (from graph) are similar to the present model values shown in Fig. 4. Variously modeled ΔH functions for the solid phase by [35Sca], [37Bor], [38Wic], [49Wic], [53Har], [60Tool], [71Kub], [71Hay], [73Car], and [81Pel (from graph)] together with the experimentally determined values by [70Jon] and the estimated value of [76Mac] from short-range order coefficients are shown in Fig. 5.

Present Thermodynamic Evaluation of the Phase Diagram. The lattice stability parameters given in Table 7 for pure Au and Pt were derived from the heats of transformation [83Cha] at the melting point (ΔH(Au) = 13 000 J/mol, ΔH(Pt) = 19 650 J/mol) and by assuming $\Delta C_p = 0$ for both components. Because of the lack of experimental basis for the thermodynamic modeling, only simple expressions for the excess Gibbs energy function

Fig. 5 Comparison of Composition Dependence of $\Delta H/X(1 - X)$

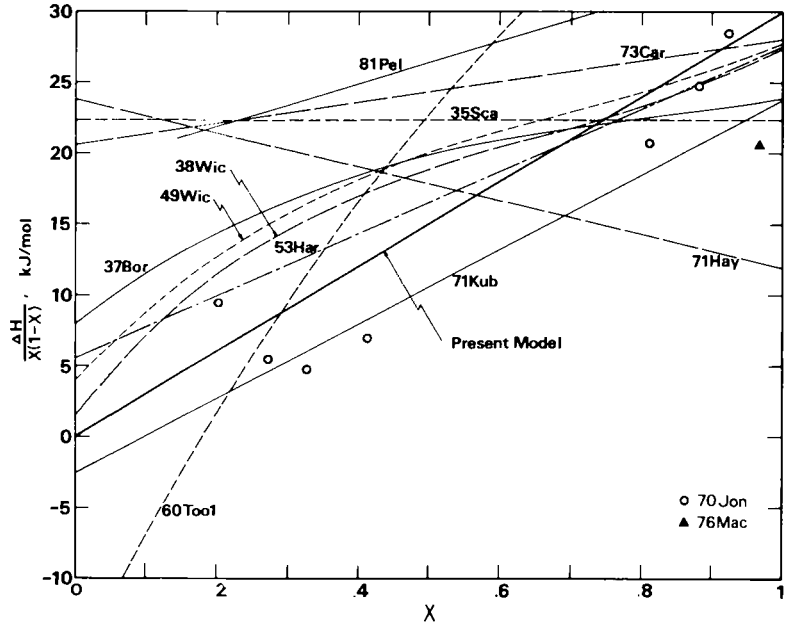

X is the atomic fraction of Pt.

H. Okamoto and T. B. Massalski, 1985.

Table 7 Thermodynamic Functions for the Liquid and Solid Phases

Reference	Enthalpy of mixing, $\left(\frac{\Delta H}{X(1-X)}\right)$, J/mol	Excess entropy of mixing, $\left(\frac{\Delta S^{ex}}{X(1-X)}\right)$, J/mol·K
Liquid phase		
[35Sca].....	22 096	0
[73Car].....	24 560 − 368 X	0
[80Mie].....	17 000 + 1 000 X	...
[80Pel].....	5 200	~0
Present model.....	23 500 + 4 000 X	0
Solid phase		
[35Sca].....	22 270	0
[37Bol].....	7 900 + 40 320 X − 40 320 X^2 + 16 210 X^3	0
[38Wic].....	1 372 + 62 560 X − 71 870 X^2 + 35 290 X^3	0
[49Wic].....	3 949 + 55 040 X − 60 650 X^2 + 29 510 X^3	0
[53Har].....	5 523 + 22 092 X	−9.73 + 9.73 X
[60Too1].....	−16 608 + 98 296 X − 39 296 X^2	−12.739 + 37.626 X − 9.4331 X^2
[71Hay].....	28 360 − 11 930 X	...
[71Kub].....	−2 653 + 26 464 X	−14.64 + 10.88 X
[73Car].....	20 640 + 7 372 X	0
Present model.....	30 000 X	−13.00 + 14.183 X

Note: X is atomic fraction of Pt. ΔH and ΔS^{ex} were assumed to have no temperature dependence.

Lattice stability parameters, J/mol

$G^0_L(\text{Au}) = 0$
$G^0_L(\text{Pt}) = 0$
$G^0_s(\text{Au}) = -13\,000 + 9.7190\,T$
$G^0_s(\text{Pt}) = -19\,650 + 9.6224\,T$

have been assumed here in the form $\Delta G^{ex}_s = X(1 - X) \cdot (A + BX - (C + DX)T)$ for the solid phase and $\Delta G^{ex}_L = X(1 - X)(E + FX)$ for the liquid phase.

It appears that the Au-rich side of the miscibility gap boundary goes through $X = 0$, or intersects the composition axis at a slightly positive side when the temperature, T, is extended to 0 K. Therefore, the $\Delta H/X(1 - X)$ function is likely to be zero or negative at $X = 0$. Only the models by [60Too1] and [71Kub] satisfy this condition. The model by [71Kub] shows a narrow miscibility gap and the critical point at a temperature that is too high. The ΔH function by [60Too1] (Fig. 5) appears to be changing too rapidly with composition. It was assumed in the present model that $\Delta H/X(1 - X)$ is 0 at $X = 0$. The term linear with the composition in the $\Delta H/X(1 - X)$ function was taken to be $30X$ kJ/mol for the best fitting by trial and error. The excess entropy term can be calculated from the critical point of the miscibility gap. The expressions derived in the present model are given in Table 7, and Fig. 4 and 5. The parameters for the liquid phase assumed in the present model are also given in Table 7.

The calculated phase boundaries (Fig. 6) are within the experimental uncertainty limits except for a part of the liquidus near 10 at.% Pt. The calculated liquidus shows an unusual depression at about 15 at.% Pt (Fig. 6). This reflects the existence of the miscibility gap that nearly touches the solidus. (The presently assessed critical temperature is only 40 °C below the solidus.) If the solidus and the miscibility boundary actually touched to involve a peritectic reaction, the depression at 15 at.% Pt would develop into two separate branches of the liquidus having different slopes above and below the peritectic temperature. The experimental data show no clear sign of the calculated depression, but it is considered that this effect

Fig. 6 Comparison of Au-Pt Assessed and Calculated Phase Boundaries

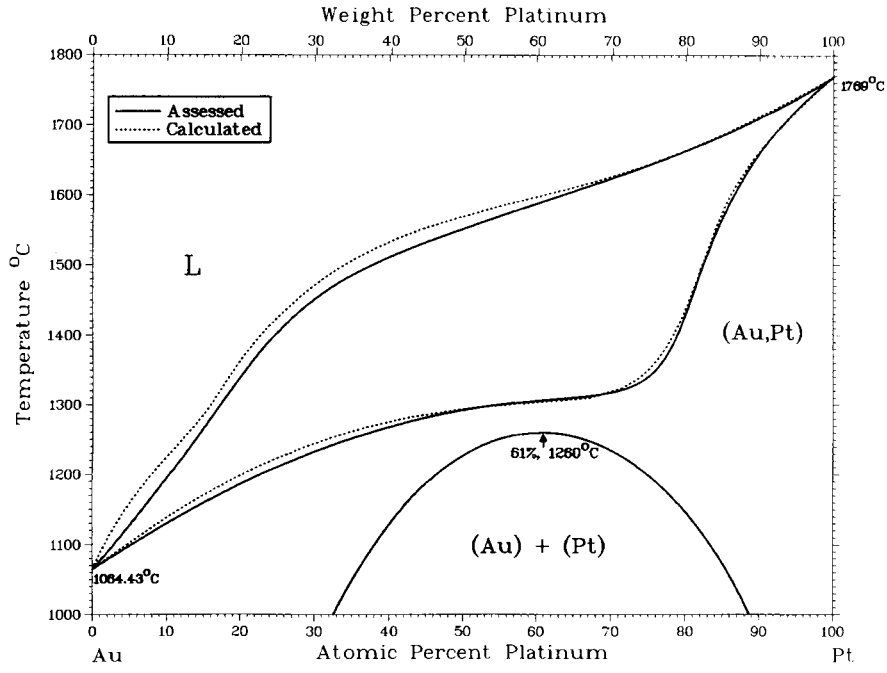

H. Okamoto and T. B. Massalski, 1985.

is real. Very careful work in this composition range should be able to demonstrate this.

Suggestions for Future Experimental Research

In the opinion of the present evaluators, the following features of the Au-Pt phase diagram may be considered to be tentative, or in need of future research:

- Both liquidus and solidus curves need reexamination because of substantial scatter (Fig. 1). No two reports in the literature are alike in detail.
- The possibility that a stable Au_3Pt phase exists should be explored further experimentally.
- Thermodynamic data for this system are scarce. More information would be beneficial as an aid in accurate calculation of phase boundaries.

The Au-Pt system, as contributed in a short version by S. P. Singhal, was published in provisional form in the *Bulletin* [81Sin]. The present evaluation reviews all bibliography and data on the Au-Pt system available in the literature through 1982 and includes information pertaining to the crystal structures, metastable phases, and thermodynamics. The present authors have also performed a thermodynamic assessment of certain phase boundaries. The present evaluation may be considered as superseding the earlier work.

Cited References

***07Doe:** F. Doerinckel, "Several Platinum Alloys", *Z. Anorg. Chem., 34,* 333-366 (1907) in German. (Equi Diagram; Experimental; #)

28Gri: A. T. Grigorjew, "The Gold-Platinum Alloys", *Ann. Inst. Platine (Leningrad), 6,* 184-194 (1928) in Russian; *Z. Anorg. Chem., 178,* 97-107 (1929) in German. (Equi Diagram; Experimental; #)

***30Joh:** C. H. Johansson and J. O. Linde, "Crystal Structures, Electrical Resistance, Thermal Forces, Heat Conductivity, Magnetic Susceptibility, Hardness, and Tempering Phenomena in the System Gold-Platinum in Relation to the Phase Diagram", *Ann. Phys., 5*(6), 762-792 (1930) in German. (Equi Diagram, Crys Structure, Meta Phases; Experimental; #)

31Ste: W. Stenzel and J. Weerts, "X-Ray Examination of Alloys of the Gold-Platinum System", Festschrift zum 50-jahrigen Bestehen der Platinschmelze, G. Siebert G.m.b.H., 300-308 (1931) in German. (Equi Diagram; Experimental; #)

32Wee: J. Weerts, "Precise X-Ray Process in Alloy Research", *Z. Metallkd., 24*(6), 139-140 (1932) in German. (Equi Diagram; Experimental; #)

34Sel: H. Seltz, "Thermodynamics of Solid Solutions. I. Perfect Solutions", *J. Am. Chem. Soc., 56*(2), 307-311 (1934). (Thermo; Theory)

35Sca: G. Scatchard and W. J. Hamer, "The Application of Equations for the Chemical Potentials to Equilibria Between Solid Solution and Liquid Solution", *J. Am. Chem. Soc., 57,* 1809-1811 (1935). (Thermo; Theory)

35Sel: H. Seltz, "Thermodynamics of Solid Solutions. II. Deviation from Raoult's Law", *J. Am. Chem. Soc., 57*(3), 391-395 (1935). (Thermo; Theory)

37Bor: G. Borelius, "The Theory of the Transformation of Metallic Mixed Phases. IV. The Separation of Disordered Mixed Phases", *Ann. Phys., 28,* 507-519 (1937) in German. (Equi Diagram, Thermo; Theory)

37Joh: C. H. Johansson and O. Hagsten, "Proof of Hysteresis Between the Dissociation and Reformation of the Homogeneous Metal Phase", *Ann. Phys., 28,* 520-527 (1937). (Equi Diagram; Theory)

38Bor: G. Borelius, "The Theory of the Transformation of Metallic Mixed Phases. V. Fluctuation and Nucleus Formation in Undercooled Phases", *Ann. Phys., 33,* 517-531 (1938) in German. (Equi Diagram; Theory)

38Wic: C.G. Wictorin, "The Separation of Gold-Platinum Alloys", *Ann. Phys., 33,* 509-516 (1938) in German. (Equi Diagram, Thermo; Experimental; #)

47Wic1: C.G. Wictorin, "Studies in Gold Platinum Alloys", Stockholm, Ivar Hoeggstrom (1947) cited in [52Har, 53Har]. (Equi Diagram; Experimental; #)

47Wic2: C.G. Wictorin, Dissertation, University of Stockholm (1947) as cited in [Hansen]. (Equi Diagram; Experimental; #)

49Wic: C.G. Wictorin, "Two-Phase Boundary of the Au-Pt System", *Arkiv Mat. Astron. Fys., B36*(9), 509-516 (1949). (Equi Diagram, Thermo; Experimental; #)

51Bor: G. Borelius, "Kinetics of Precipitation in Supercooled Solid Solutions", *Trans. AIME, 191,* 477-484 (1951). (Equi Diagram; Theory)

***51Gru:** G. Grube, A. Schneider, and U. Esch, "Gold-Platinum System", Festschrift aus Anlass des 100-jahrigen Jubilaums der Firma, W.C. Heraeus G.m.b.H., 20-42 (1951). (Equi Diagram, Crys Structure, Meta Phases; Experimental; #)

***52Dar:** A.S. Darling, R.A. Mintern, and J.C. Chaston, "The Gold-Platinum System," *J. Inst. Met., 81,* 125-132 (1952-1953). (Equi Diagram, Crys Structure; Experimental; #)

52Har: H.K. Hardy, "Discussion; The Gold-Platinum System", *J. Inst. Met., 81,* 599-600 (1952-1953). (Thermo; Theory)

53Har: H.K. Hardy, "A 'Sub-Regular' Solution Model and Its Application to Some Binary Alloy Systems", *Acta Metall., 1*(3), 202-209 (1953). (Thermo; Theory)

55Rau: E. Raub and G. Worwag, "The Gold-Platinum-Palladium Alloys", *Z. Metallkd., 46*(7), 513-515 (1955) in German. (Crys Structure; Experimental)

57Tie: T.J. Tiedema, J. Bouman, and W.G. Burgers, "Precipitation in Gold-Platinum Alloys", *Acta Metall., 5,* 310-321 (1957). (Equi Diagram, Meta Phases; Experimental; #)

58Wei: R.J. Weiss and K.J. Tauer, "Thermodynamics of the Au-Pt System", *J. Phys. Chem. Solids, 7,* 249 (1958). (Thermo; Theory)

60Mun: A. Munster and K. Sagel, "Separation Curve and Critical Point of the System Gold-Platinum", *Z. Phys. Chem. (Frankfurt), 23*(56), 415-425 (1960) in German. (Equi Diagram; Experimental; #)

60Too1: L.J. van der Toorn and T.J. Tiedema, "Precipitation in Gold-Platinum Alloys—I. Thermodynamics", *Acta Metall., 8,* 711-714 (1960). (Thermo; Theory)

60Too2: L.J. van der Toorn, "Precipitation in Gold-Platinum Alloys—II. Influence of the Spinodal Curve on the Rate and the Mechanism of the Precipitation Process", *Acta Metall., 8*(10), 715-727 (1960). (Equi Diagram; Experimental)

61Mei: J.L. Meijering, "On the Thermodynamics of the Au-Pt System", *J. Phys. Chem. Solids, 18,* 267-268 (1961). (Thermo; Theory)

61San: V.V. Sanadze and N.I. Labartkava, "Phase Transitions in the Gold-Platinum System", *Zh. Struct. Khim., 2,* 703-711 (1961) in Russian; TR: *J. Struct. Chem., USSR, 2,* 647-654 (1961). (Meta Phases; Experimental)

62Dar: A.S. Darling, "Gold-Platinum Alloys. A Critical Review of Their Constitution and Properties", *Platinum Met. Rev., 6*(2), 60-67 (1962). (Equi Diagram; Review); *6*(3), 106-111 (1962). (Equi Diagram; Review)

64Rau: E. Raub and G. Falkenburg, "The System Gold-Platinum-Rhodium and the Binary Systems of Its Components", *Z. Metallkd., 55,* 392-397 (1964) in German. (Equi Diagram, Meta Phases: Experimental; #)

65Coo: H.E. Cook and J.E. Hilliard, "A Simple Method of Estimating the Chemical Spinodal", *Trans. AIME, 233*(1), 142-146 (1965). (Equi Diagram; Theory)

65Def: D. deFontaine and J.E. Hilliard, "Comment on 'Precipitation in Gold-Platinum Alloys: Thermodynamics'", *Acta Metall., 13*(9), 1019-1021 (1965). (Thermo; Theory)

67Car: R.W. Carpenter, "Growth of Modulated Structure in Gold-Platinum Alloys", *Acta Metall., 15,* 1567-1572 (1967). (Equi Diagram, Crys Structure; Experimental)

67Fie: R. Fiedler, "X-Ray 'Tails' on Powder Patterns of Annealed Au-Pt and Fe-Ni Alloys", *Czech. J. Phys., 17*(12), 1105-1109 (1967). (Meta Phases; Experimental)

68Gol: E. Gold and E.S. Machlin, "A Field Ion Microscope Investigation of Short-Range Order in 2 at.% Au-Pt and 2 at.% Ni-Pt", *Philos. Mag., 18*(153), 453-464 (1968). (Crys Structure; Experimental)

68Wei: V.J. Weise and V. Gerold, "Coherent and Incoherent Precipitation in the Au-Pt System", *Z. Metallkd., 59*(12), 904-909 (1968) in German. (Meta Phases; Experimental)

69Kra: G. Kralik, J. Weise, and V. Gerold, in *The Mechanism of Phase Transformations in Crystalline Solids,* Inst. Metals, London, 23-28 (1969). (Meta Phases; Experimental)

***70Jon:** R.W. Jones, F.E. Stafford, and D.H. Whitmore, "Mass Spectrometric Study of the Thermodynamic Properties of Solid Au-Pt Alloys", *Met.* Trans., 1(2), 403-413 (1970). (Thermo; Experimental)

70Kra: G. Kralik, "Investigation on the Decomposition Kinetics of Gold-Platinum Alloys by Means of Electrical Resistivity", *Z. Metallkd., 61*(10), 751-756 (1970) in German. (Equi Diagram, Meta Phases; Theory)

71Bor: G. Borelius, "Spinodal Hypotheses and Precipitation in AuPt and AuNi Alloys", *Phys. Scr., 4*(3), 127-131 (1971). (Equi Diagram; Theory)

71Hay: F.H. Hayes and O. Kubaschewski, "The Heats of Formation in the System Gold-Platinum-Palladium", *Mat. Sci. J., 5*(1), 37-40 (1971). (Thermo; Experimental)

71Kub: O. Kubaschewski and J.F. Counsell, "Thermodynamic Properties of the Gold-Platinum-Palladium System", *Monatsh. Chem., 102*(6), 1724-1728 (1971) in German. (Thermo; Theory)

73Car: S.M. Carmio and J.L. Meijering, "The Gold-Nickel-Platinum System", *Z. Metallkd., 64*(3), 170-175 (1973) in German. (Thermo; Theory)

74Pol: W. Polanschutz and E. Krautz, "Field Ion Microscopic Investigations in the Binary System Platinum-Gold", *Surf. Sci., 46*(2), 602-610 (1974). (Meta Phases; Experimental)

75Che: C.G. Chen and R.W. Balluffi, "Field Ion Microscope Studies of Solute Atoms in Dilute Pt Alloys—II. Distributions and Interactions of Au and Ni Atoms", *Acta Metall., 23*(8), 931-936 (1975). (Crys Structure; Experimental)

76Mac: E.S. Machlin, "On Previous Field Ion Microscope Measurements of Short Range Order in Dilute Alloys of Platinum", *Scr. Metall., 10*(6), 521-524 (1976). (Crys Structure, Thermo; Review)

78Dek1: T.H. deKeijser, "The Structure of Spinodally Decomposed Pt-Rich AuPt Alloys", *Acta Crystallogr. A, 34*(S4), S302 (1978). (Equi Diagram; Experimental)

78Dek2: T.H. deKeijser and J.L. Meijering, "The Estimation of Chemical Spinodal", *Scr. Metall., 12*(9), 843-846 (1978). (Equi Diagram; Theory)

78Sav: E.M. Savitsky, V.P. Polyakova, N.B. Gorina, and N.R. Roshan, *Physical Metallurgy of Platinum Metals,* Pergamon Press, Elmsford, NY (1978). (Equi Diagram; Review)

78Sin1: S.P. Singhal, H. Herman, and J.K. Hirvonen, "Spinodal Decomposition in Amorphous Au-Implanted Pt", *Appl. Phys. Lett., 32*(1), 25-26 (1978). (Meta Phases; Experimental)

78Sin2: S.P. Singhal, H. Herman, and G. Kostorz, "Neutron Small-Angle Scattering Study of Phase Decomposition in Au-Pt", *J. Appl. Crystallogr., 11*(5), 572-577 (1978). (Equi Diagram; Theory)

79Mul: H.U. Muller, "Contribution to the Thermodynamics of Binary Alloys", thesis, Tech. Univ. Aachen (1979) in German. (Thermo; Theory)

79Sch: H.J. Schaller, "A Thermodynamic Analysis of the Pt-Au Miscibility Gap", *Z. Metallkd., 70*(6), 354-358 (1979) in German. (Thermo; Theory)

80Mie: A.R. Miedema, P.F. deChatel, and F.R. deBoer, "Cohesion in Alloys—Fundamentals of a Semi-Empirical Model", *Physica, 100B,* 1-28 (1980). (Thermo; Theory)

80Ovc: A.A. Ovcharenko, "Computer Calculation of the Constitution Diagrams of Certain Binary Alloys with Determination of Interaction Parameters from Experimental Diagrams", *Fiz. Met. Metalloved., 49*(5), 1013-1020 (1980) in Russian; TR: *Phys. Met. Metallogr., 49*(5), 96-102 (1980). (Thermo; Theory)

80Sin: S.P. Singhal, Ph.D. thesis, State University of New York at Stony Brook (1980). (Meta Phases; Theory)

81Pel: A.D. Pelton, H. Kohler, and A. Dubreuil, "Some Useful Thermodynamic Relationships Involving Binary Phase

Diagrams", *Chemical Metallurgy, a Tribute to Carl Wagner,* 23-25 (1981). (Thermo; Theory)

81Sin: S. P. Singhal, "The Au-Pt (Gold-Platinum) System", *Bull. Alloy Phase Diagrams, 2*(1), 66-70 (1981). (Equi Diagram, Meta Phases; Review)

83Cha: M. W. Chase, "Heats of Transformation of the Elements", *Bull. Alloy Phase Diagrams, 4*(1), 123-124 (1983). (Thermo; Compilation)

*Indicates key paper.
#Indicates presence of a ph ıse diagram.

Au-Pt evaluation contributed by **H. Okamoto** and **T. B. Massalski,** Department of Metallurgical Engineering and Materials Science, Carnegie-Mellon University, Pittsburgh, PA 15213, USA. Work was supported by the International Gold Corporation Limited (InterGold) and American Society for Metals (ASM). Literature searched through 1983. Part of the bibliographic search was provided by ASM. Professor Massalski is the ASM/NBS Data Program Editor-in-Chief for the Binary Alloys, and also Category Editor for binary gold alloys, jointly with Dr. Okamoto.

The Mg-Pb (Magnesium-Lead) System

24.305 207.2

By A. A. Nayeb-Hashemi and J. B. Clark
University of Missouri-Rolla

Equilibrium Diagram

The equilibrium phase diagram of the Mg-Pb system was determined by several investigators [05Gru, 05Kur, 65Dob, 65Eld]. The general characteristics of the Mg-Pb equilibrium diagram as given in [Hansen] are well established and agreed upon. The equilibrium diagram of the Mg-Pb system modified by the work of [65Eld], which also has appeared in compilations of [Shunk], [Metals Handbook], and [Hultgren, Binary], has not been unequivocally confirmed. (See "Liquidus".)

The assessed equilibrium Mg-Pb phase diagram shown in Fig. 1 includes: (1) L, the liquid; (2) (Mg), the terminal Mg solid solution with a maximum solid solubility of 7.75 at.% Pb (41.73 wt.% Pb); (3) Mg_2Pb, the stoichiometric intermetallic compound with a cubic antifluoride structure; (4) (Pb), the terminal Pb solid solution with a maximum solid solubility of 6 at.% Mg (94 at.% Pb); and (5) two eutectic reactions, one at 19.1 at.% Pb and one at 83 at.% Pb. (See Table 1.)

Figure 2 shows the data for the liquidus, solidus, and the solvus boundaries taken from the ten principal studies of the system, along with the calculated boundaries.

Liquidus. The first thermal analysis of Mg-Pb alloys was done by measuring the effect of Mg on the freezing point of

Fig. 1 Mg-Pb Assessed Phase Diagram

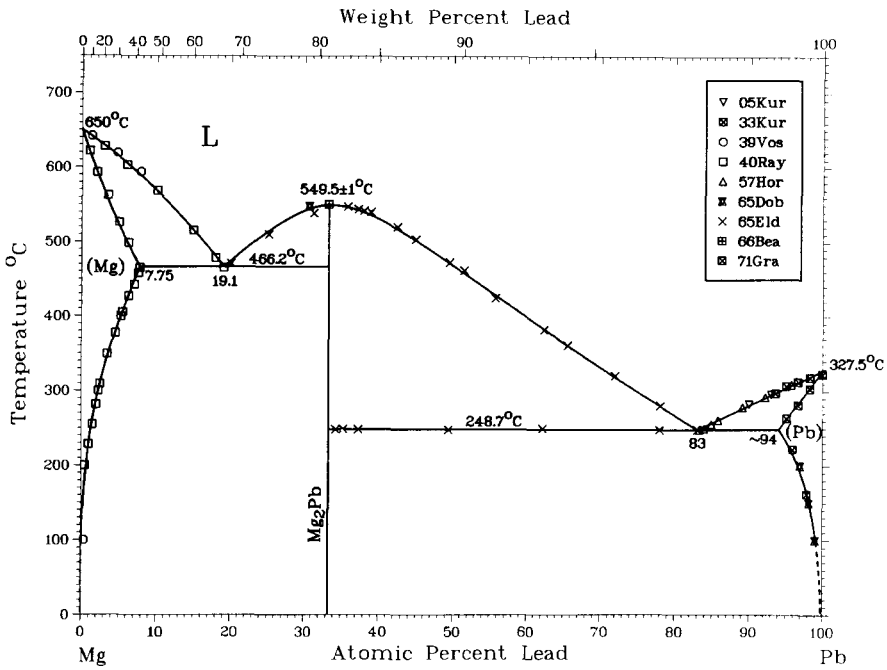

Selected experimental data are shown.

A. A. Nayeb-Hashemi and J. B. Clark, 1985.